Ab initio Molecular Dynamics Simulations of Field-Coupled Nanocomputing Molecules

Y. Ardesi[1], A. Gaeta[1], G. Beretta[1], G. Piccinini[1] and M. Graziano[2]

[1] Department of Electronics and Telecommunications, Politecnico di Torino, Torino, Italy.
[2] Department of Applied Science and Technology, Politecnico di Torino, Torino, Italy
e-mail: yuri.ardesi@polito.it

***Abstract*— Molecular Field-Coupled Nanocomputing (FCN) represents one of the most promising solutions to overcome the issues introduced by CMOS scaling. It encodes the information in the molecule charge distribution and propagates it through electrostatic intermolecular interaction. The need for charge transport is overcome, hugely reducing power dissipation. At the current state-of-the-art, the analysis of molecular FCN is mostly based on quantum mechanics techniques, or ab initio evaluated transcharacteristics. In all the cases, studies mainly consider the position of charges/atoms to be fixed. In a realistic situation, the position of atoms, thus the geometry, is subjected to molecular vibrations. In this work, we analyse the impact of molecular vibrations on the charge distribution of the 1,4-diallyl butane. We employ Ab Initio Molecular Dynamics to provide qualitative and quantitative results which describe the effects of temperature and electric fields on molecule charge distribution, taking into account the effects of molecular vibrations. The molecules are studied at near-absolute zero, cryogenic and ambient temperature conditions, showing promising results which proceed towards the assessment of the molecular FCN technology as a possible candidate for future low-power digital electronics. From a modelling perspective, the diallyl butane demonstrates good robustness against molecular vibrations, further confirming the possibility to use static transcharacteristics to analyse molecular circuits.**

***Index Terms*— Field-Coupled Nanocomputing; Molecular Dynamics; Charge Dynamics; Electrostatic Intermolecular Interaction; Beyond-CMOS.**

I. Introduction

The improvement of digital electronics performance in the last decades has been made possible by the well-known scaling process of CMOS technology. At state of the art, the size of single transistors is approaching the molecular scale, posing serious concerns about the possibility of continuing to cope with current research challenges by employing scaling techniques only. For this reason, researchers and scientists are proposing many technologies alternative to CMOS which base the computing paradigm on novel physical phenomena. This is well-known as the beyond-CMOS. Field-Coupled Nanocomputing is one of the most promising solutions: it propagates the information without current transport, extremely reducing the power dissipation. Among the possibilities, Molecular FCN encodes the information in the charge configuration of molecules, see Fig. 1(a), and allows the computation through electrostatic intermolecular interaction [1].

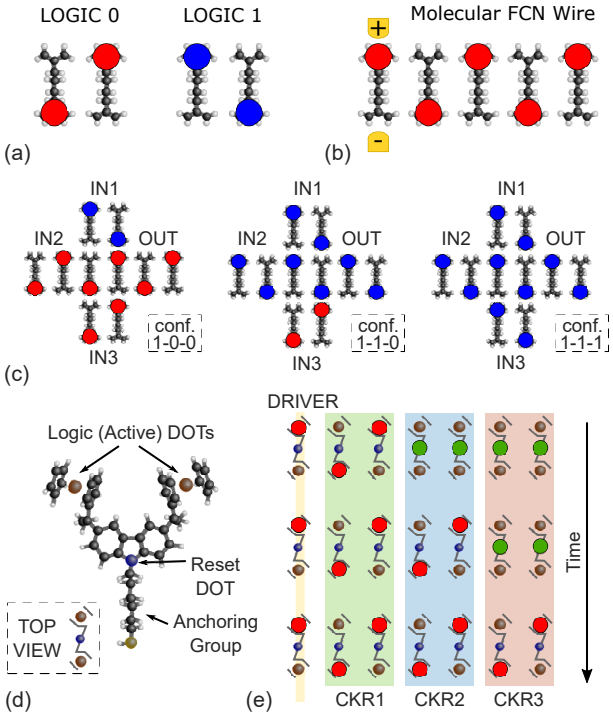

Fig. 1: Molecular FCN basics: (a) encoding of the binary information in a molecular cell based on oxidised diallyl butane molecules. The red and blue circles represent the position of the oxidation charges in the molecules encoding '0' and '1' respectively. (b) Molecular FCN wire. The first molecule is driven by external metal electrodes which force the polarisation of the first molecule, acting as molecular wire input. (c) Molecular FCN majority voter in three possible configurations; not shown configurations are electrostatically equivalent to reported ones. (d) Bis-ferrocene molecule. (e) Molecular FCN wire subdivided into three clock regions (CKR1, CKR2, and CKR3). When the clock is active, the information is encoded by active dots (red circles), making propagation possible. The charge is pushed in the reset dot when the clock is de-activated.

At the current state-of-the-art, the molecular FCN literature often relies on the Quantum-dot Cellular Automata (QCA) concept. It models the molecular cell as an ideal element composed of four quantum dots with two mobile charges. This system can be analysed through quantum mechanics by using the so-called two-state approximation [2, 3]. This method permits the analysis of the information propagation [4], and the energy dissipation [5] in general QCA circuits. In recent studies, we started analysing the molecule considering its effective physical behaviour, by exploiting the so-called MosQuiTo (Molecular Simulator Quantum-dot cellular automata Torino) methodology [6, 7]. This methodology allows to formulate considerations that link the physical characteristics of the molecule with the

Digital Object Identifier 10.29292/jics.v16i1.474

system-level circuit analysis [8, 9, 10]. In the literature, molecules are generally considered static elements which vary their charge distribution as a consequence of the interaction with external stimuli [7, 2]. In a realistic situation, the position of atoms, thus the geometry, might be subjected to an oscillating motion due to molecular vibrations. Moreover, molecular FCN is often conceived as a possible FCN technology working at ambient temperature. As molecular vibrations are typically amplified by temperature, the study of molecular vibration effects becomes essential to understand whether computation is possible at ambient temperature.

This paper analyses the impact of molecular vibrations on the charge distribution of possible FCN molecules. Sec. II. summarises the basics of molecular FCN technology, then in Sec. III., we propose a methodology embedded in the MoSQuiTo method and based on Ab Initio Molecular Dynamics (AIMD) to study the effects of molecular vibrations. In Sec. IV., we use the proposed methodology to study how the molecular vibrations impact on the charge distribution of molecules. We validate the methodology in the simplest case of water. Then, we study the effects of temperature and electric fields in a more realistic solution. We analyse the 1,4-diallyl butane, a molecule which is often used to characterise the essential interaction in molecular FCN [1]. Finally, in Sec. V. we discuss the qualitative and quantitative results. The obtained results provide important feedback both from a modelling and a practical perspective. We confirm the validity of static methodologies, and we proceed towards the assessment of molecular FCN technology as a possible candidate for digital electronics working at ambient temperature.

II. Background

A. Molecular Field-Coupled Nanocomputing paradigm

Among the beyond-CMOS possible paradigms proposed to overcome the well-known scaling issues, Field-Coupled Nanocomputing is one of the most interesting. Nanometric objects encode the information in some physical quantities such as charge or magnetization. Local-field interaction allows the information to propagate element-by-element, without the need for charge transport. The absence of electrical current drastically decreases the power dissipation, whereas the very small size of single elements permits a very high density of devices on the single chip. These two benefits make this technology very promising for low-power digital electronics.

Many technologies have been proposed to implement the FCN. For example, the magnetic FCN paradigm encodes the information in the magnetization of nanometric magnets and propagates it through magnetic interaction [11, 12]. This work analyses molecular FCN technology: the charge distribution of molecules defines the logic information whereas the electrostatic intermolecular interaction enables the information to propagate. The information encoding of molecular FCN is generally based on the so-called Quantum-dot Cellular Automata paradigm. Two oxidized molecules are juxtaposed to create a square-shaped molecular QCA cell. The two oxidation charges tend to repel each other, thus creating two possible configurations used to encode the two logic states, see Fig. 1(a). In a few cases, single molecules possess all the four dots, creating a single-molecule molecular QCA cell [13].

B. Molecular FCN devices

The electrostatic interaction among molecular cells allows the information to propagate, enabling the conception of molecular wires, see Fig. 1(b). The first molecule locates between two electrodes that force its polarization. The first molecule acts as a driver for the wire and imposes the propagated binary information. The same electrostatic interaction also enables computing. Fig. 1(c) shows a possible majority voter. Three cells (top, left and bottom) define the inputs of the 3-bit majority voter, the central cell allows the voting mechanism and, to achieve the electrostatic energy minimization, copies the logic of the most recurrent logic. Eventually, the logic is copied to the output (right) cell. Inverter and more complex FCN devices have been also proposed in the literature [14, 15, 16].

C. Clocking mechanism

The electrostatic interactions among adjacent molecules play a key role in enabling the elaboration and propagation of digital information. Despite the electric fields generated by molecules last after a few nanometers, all molecules interact with each other, with different strength, independently on their position. A clocking mechanism is typically employed to introduce a pipelining mechanism that guides the intermolecular interaction. The clock activates or inhibits some molecule regions (clock regions) so that the propagation can be correctly achieved. The clock mechanism is made possible by using molecules with more than two dots (reset dot), for instance, the bis-ferrocene molecule [17, 18], shown in Fig. 1(d). Fig. 1(e) shows the propagation of the information in a bis-ferrocene clocked molecular wire.

III. Methodology

A. MosQuiTo Methodology

In the field of FCN technology, devices are based on non-conductive physical phenomena (e.g. electrostatic or magnetic interactions) which strongly impact on the propagation and elaboration of the digital information. For these reasons, FCN devices require vertical methodologies which allow designers to evaluate the system-level implications of physical parameters correctly. This lead to the essential requirement of methodologies which are strongly linked with the physical characteristics of devices, enabling the correct analysis and design of devices based on emerging technologies [19, 20, 21].

In this paper, we focus on Molecular FCN. This technology can be analysed using the so-called MosQuiTo methodology (Molecular Simulator Quantum-dot cellular automata Torino) [7, 6]. It consists of a three-step procedure subdivided into molecule characterisation, figures of merit extraction, and system-level analysis.

Molecule Characterisation: the molecule is firstly analysed to study its electrostatic behaviour. At this purpose, complex ab initio calculation evaluates how the charge distribution of the molecule changes when subjected to external stimuli. Typically, the atomic charges are obtained by fitting the molecular electrostatic potential in order to model

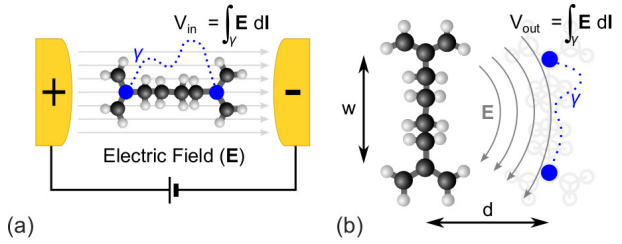

Fig. 2: Figures of merits for molecular FCN technology: (a) definition of input voltage, the molecule is embedded in an electric field generated by two electrodes, the input voltage is obtained by integrating the field between the two active dots. (b) Definition of output voltage, the charge distribution of the molecule generates an electric field. The output voltage is evaluated as the input voltage of a fictitious molecule positioned with proper distance $d = w$.

the molecule as a distribution of point charges, each centred on molecule atoms.

Figures of merits extraction: many figures of merits which have been proposed in the literature enable considering the molecule as an electronics device, with proper input and output. Each molecule can be described, from an electrostatic standpoint, as a collection of atomic charges obtained by fitting the molecular electrostatic potential. Then, the atoms can be grouped into regions. The atomic charges into each region can be summed obtaining the so-called aggregated charge Q_i. The aggregated charges locate on molecule redox centres, in case of mixed-valence compounds, or on interesting points of the molecule. The single aggregated charge is named DOT. In particular, the DOTs associated with the encoding of the information are named active dots.

The aggregated charge depends on the electric field influencing the single-molecule. In fact, a molecule is polarised when embedded in an electric field, which can be generated by an external electrode, i.e. a driver or clock system [22, 23], or other molecule charge distributions, i.e. in the information propagation mechanism. The effect of the electric field can be measured with the so-called Input Voltage V_{in}, which can be obtained by integrating the electric field $\mathbf{E}$ influencing the molecule on an arbitrary path (γ) connecting the active dots of the molecule, see Fig. 2(a). The aggregated charge enables computing the electric field generated by the molecule, potentially influencing other molecules (i.e. input voltage of other molecules). The output voltage V_{out} of a specific molecule is defined as the input voltage of a fictitious molecule juxtaposed to it with intermolecular distance (d) equal to the distance between active dots (w), see Fig. 2(b). In the first step of the MosQuiTo methodology, the atomic charges, thus the aggregated charge distribution, are evaluated for different external electric fields (i.e. different V_{in}). The aggregated charges Q_i and the input voltage V_{in} are linked together to obtain the so-called Vin-Aggregated Charge Transcharacteristics (VACT). The aggregated charge can be exploited to evaluate the output voltage of a molecule, thus the Vin-Vout Transcharacteristics (VVT).

System-level analysis: once the molecule is described with a proper VACT, each molecule can be treated as an electronic device. In particular, each molecule receives, as input voltage, a fraction of the output voltage of every molecule in the molecular circuit. The input voltage induces a precise charge on the molecule, computed with the VACT, which, in turn, generates an electric field influencing all the other molecules of the circuit. An iterative algorithm, named Self-Consistent Electrostatic Potential Algorithm (SCERPA), evaluates the charge distribution of the entire circuit by exploiting a self-consistent procedure [8]. The algorithm bases the evaluation on ab initio characterisation, thus the results are precise even if obtained in a short time.

B. Ab Initio Molecular Dynamics

This work mainly focuses on the analysis of molecules under the dynamic regime. For this reason, we exploit the so-called Ab Initio Molecular Dynamics (AIMD). This tool enables the study of geometry variation in molecules, without the need for force field databases. Indeed, the atoms are moved by exploiting gradients which are evaluated by solving, in an approximate way, the Schröedinger equation (Born–Oppenheimer Molecular Dynamics Simulation).

In this work, we make use of the ORCA free ab initio package [24, 25]. Considering the structure of the studied molecules, we perform DFT calculations using the Kohn-Shann Scheme. According to the molecules analysed in this work, CAM-B3LYP and TZVP are chosen as proper DFT functional and basis set and D3 corrections are exploited [26, 27]. The molecules are studied under the effect of different temperatures, running Molecular Dynamics calculation within the NVT ensemble (i.e. keeping the number of atoms, the volume and the temperature constant). At this purpose, a Berendsen thermostat with a time constant of 10.0 fs is used to control the temperature, thus the coupling between the molecule and the system.

IV. Results

In this section, we report the analysis of two molecules. At first, we analyse the water molecule as a mean of validating the methodology. Indeed, the water molecule is simple to analyse with DFT calculation, and the results can be easily compared with experimental and literature results. Secondly, we analyse the 1,4-diallyl butane cation. Among all the molecules proposed for FCN computation, this is the simplest one, and it is a suitable candidate for modelling and basic phenomena studies. Indeed, it permits the analysis of the physical characteristics through ab initio tools in a reasonable time.

A. Equilibrium analysis of the water molecule

The geometry of water is firstly obtained with a DFT optimisation procedure. Fig. 3(a) reports the geometry with corresponding atom names and atomic charges. In particular, we evaluate the atomic charges of the molecules obtained by fitting the electrostatic potential. The charge associated with the oxygen atom is -0.782 a.u. whereas it is 0.391 a.u. for hydrogen atoms. The two hydrogen atoms have the same atomic charge. This result is consistent with expectations. Indeed, the water molecule shows a C_{2v} symmetry which implies a net dipole moment can be present along the principal molecular axis only, see Fig. 3(a). The charge of hydrogen atoms is positive; this can be justified by the high electronegativity of the oxygen, which tends to attract electrons more than hydrogen. Oxygen electronegativity is 3.44

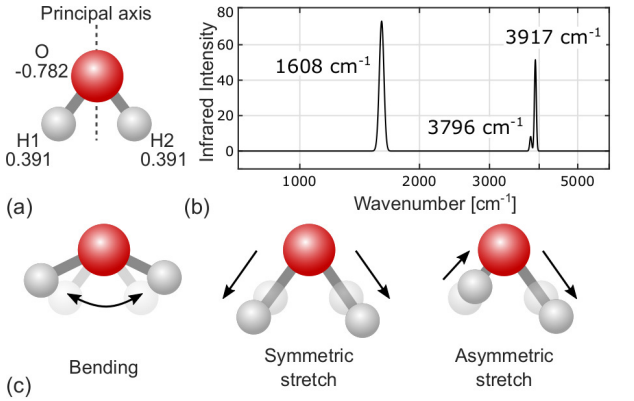

Fig. 3: Ab initio Molecular Dynamics (AIMD) analysis of the water molecule: (a) Geometry of water molecule with obtained atomic charges. (b) Infrared spectrum showing the three vibrational peaks of the molecule. (c) Geometry representation of the three water vibrational modes.

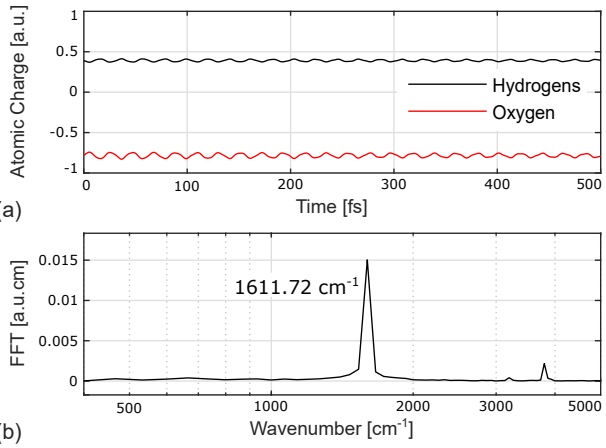

Fig. 4: Dynamics of water molecule: (a) Oxygen and hydrogen (H1) atomic charges evaluated with Ab Initio Molecular Dynamics at 350 K. The H2 atom charge is not shown for the sake of clarity, it is equal to the H1 atom charge. (b) Fast-Fourier Transform (FFT) evaluated for the oxygen atom charge.

(Pauling units), whereas hydrogen electronegativity is 2.20 (Pauling units) [28]. Notice that the sum of all the charges is null. This result is also obvious, as the molecule is neutral.

B. The vibrational spectrum of water molecule

In this work, we want to evaluate the effects of vibrations on the charge distribution of molecules. At first, we evaluate the vibration modes of water. To be coherent with literature, we express the frequency in cm^{-1} (wavenumber), the original frequency can be retrieved considering that 1 cm^{-1} corresponds to 0.03 THz.

Fig. 3(b) reports the infrared spectrum obtained for the water molecule with the ORCA package. The figure shows three significant peaks associated with the three vibrational modes. The wavelength of the three modes is 1608 cm^{-1} (48.24 THz), 3796 cm^{-1} (113.88 THz) and 3917 cm^{-1} (117.51 THz). The obtained frequencies are comparable with literature results [29] and corresponds to the modes associated with bending, symmetric stretch and asymmetric stretch, respectively. Fig. 3(c) depicts the associated movements.

C. Charge vibrations on water molecule

We now employ Ab Initio Molecular Dynamics to study the effect of vibrations on water charge distribution at a temperature of 350 K. Fig. 4(a) shows the trend of atomic charges on a 500 fs time interval. The oxygen atom charge oscillates about a 0.784 a.u. mean value with a standard deviation of 0.025 a.u.. The hydrogen atoms oscillate with a standard deviation of 0.012 a.u. about 0.392 a.u. average charge. The obtained mean values are very similar to equilibrium charges obtained in Subsec. IV.A. These results are consistent with the considerations mentioned above on molecule symmetry and electronegativity. At a temperature of 350 K, the water seems robust against molecular vibrations.

To better analyse the dynamics of charge distribution, we evaluate the Fast-Fourier Transform (FFT) of the oxygen charge. Fig. 4(b) shows the obtained frequency analysis. Three main peaks appear in the spectrum. It is interesting to note that the peaks have frequencies comparable with the vibration frequencies. This suggests vibrations are the cause of oscillations in the molecular charge distribution. The most prominent peak is centred at 1611.72 $\text{cm}^{-}1$ (48.35 THz), that is very similar to the previously obtained peak associated with bending vibrations (1633.99 cm^{-1} - 48.24 THz).

Notice that the total charge is null and the two hydrogen atoms have a similar charge. This justifies the choice of evaluating the frequency content of the oxygen charge only. We also estimated the frequency content of hydrogen atom charges, yet it is very similar to the one shown. We do not report it for the sake of brevity and because it is not considered interesting for the scope of this work.

D. The vibration spectrum of the diallyl butane cation

Given the complexity of the oxidised 1,4-diallyl butane, the geometry of the molecule is firstly optimised with DFT analysis by exploiting a valence triple-zeta basis sets with two sets of polarisation functions CAM-B3LYP/def2-TZVPP [30]. Fig. 5(a) shows the geometry of the molecule. The molecule is therefore analysed in following investigations with CAM-B3LYP/TZVP.

Compared to water, the diallyl butane has a larger number of atoms. Therefore, an analysis of single atomic charges would be difficult to examine. For this reason, we evaluate the atomic charges of the molecule in each simulation, and then we aggregate the values according to the definition reported in Fig. 5(a) to define the so-called aggregated charge. The use of the aggregated charge simplifies the study of the molecule electrostatic behaviour. At the thermal equilibrium, the obtained aggregated charges Q_{DOT1} and Q_{DOT2} are both 0.500 a.u., demonstrating a uniformly distributed molecular charge. Also for this molecule, we evaluate the infrared spectrum, reported in Fig. 5(b). It shows several peaks which might affect the final molecule dynamics. Table I lists the most significant peaks: N is the vibrational mode number (according to ORCA package output), k is the wavenumber, whereas f is the vibrational frequency (evaluated by considering 1 cm^{-1} equal to 0.03 THz).

E. Charge vibrations of diallyl butane

To understand how vibrations influence the charge distribution of the diallyl butane, we analyse the molecule in a

Table I. Vibrational modes of the 1,4-diallyl butane

N	k [cm^{-1}]	f [THz]	N	k [cm^{-1}]	f [THz]
9	78.55	2.3565	48	1386.29	41.5887
14	317.71	9.5313	50	1415.36	42.4608
17	416.20	12.4860	52	1428.78	42.8634
19	445.05	13.3515	55	1499.81	44.9943
24	628.03	18.8409	57	1524.16	45.7248
27	897.50	26.9250	59	1545.37	46.3611
29	922.45	27.6735	60	1570.72	47.1216
34	1003.16	30.0948	63	3050.97	91.5291
35	1010.29	30.3087	66	3080.81	92.4243
36	1037.92	31.1376	67	3090.68	92.7204
37	1056.60	31.6980	69	3126.66	93.7998
42	1160.02	34.8006	70	3181.40	95.4420
45	1334.70	40.0410	76	3286.39	98.5917

500 fs timeframe by exploiting the AIMD tool. At first, the molecule is analysed at 350 K. Fig. 6(a) shows the obtained aggregated charges in the time-domain. The atomic charges are aggregated according to the definition of Fig. 5(a).

The mean values of DOT1 and DOT2 aggregated charges are $\bar{Q}_{DOT1}$=0.513 a.u. and $\bar{Q}_{DOT2}$=0.4867 a.u. respectively. Similarly to the case of the water molecule, the average charge values are very close to the ones obtained for the molecule at the equilibrium. Notwithstanding this, the standard deviation is larger, σ_Q=0.1174 a.u. both for DOT1 and DOT2. The diallyl butane appears more sensible to molecular vibration than water. By analysing the charge in the time-domain, it is possible to see that charge variation is larger than the previous case, as confirmed also by the peak values of the FFT shown in Fig. 6(b). Indeed, for the water molecule, the variation of hydrogen and oxygen charges is hardly noticeable in the time domain; in this case, the amplitude of charge oscillations is larger.

F. *Temperature effects on the diallyl butane*

One of the physical quantities which might affect the intensity of molecular vibrations, i.e. the dynamics of charge, is the temperature. We employ the AIMD tool to analyse the effects of temperature on the diallyl-butane. We study the diallyl butane molecule at several temperatures, from near-absolute zero to 350 K.

Fig. 7(a) shows the charge distribution resulting from the AIMD simulation. Vibrations and consequent charge oscillation reduce their intensity when the temperature is reduced. Charge oscillations drastically drop at low temperature (i.e. 5 K).

Tab. II reports the average value of DOT1 ($\bar{Q}_{DOT1}$) and DOT2 ($\bar{Q}_{DOT2}$) charges in the timeframe. The table also

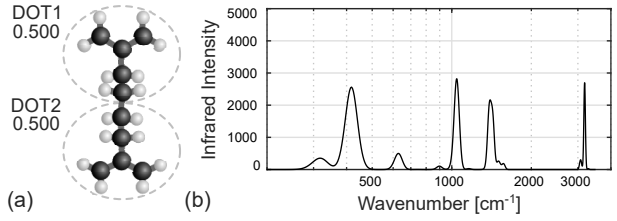

Fig. 5: Diallyl butane molecule: (a) Geometry obtained by the optimization procedure with CAM-B3LYP/TZVP. The atoms are grouped according to the definition of aggregated charge used in this article. (b) Infrared spectrum.

Table II. Temperature effects on diallyl butane charge distribution

T [K]	$\bar{Q}_{DOT1}$ [a.u.]	$\bar{Q}_{DOT2}$ [a.u.]	σ_Q [a.u.]
5	0.4994	0.5006	0.0082
50	0.5046	0.4954	0.0317
100	0.5057	0.4943	0.0470
200	0.5285	0.4715	0.0877
300	0.4973	0.5027	0.1015
350	0.5133	0.4867	0.1174

reports the standard deviation of the charge (σ_Q), which increases with temperature. This quantitative data confirm the considerations mentioned above: the two average charges are similar for all the temperatures, thus the temperature does not influence the average charge distribution of molecules. On the contrary, the temperature has a significant impact on the oscillation amplitude. The higher is the temperature, and the higher is the amplitude of charge oscillations

Fig. 7(b) shows the frequency content of the FFT of the molecule charge. It is interesting to see that the peaks are just rescaled from one temperature and the other. The position and number of peaks measured in the considered frequency span are kept fixed.

G. *Effects of electric fields*

So far, we considered the molecule to be influenced by the temperature, yet we didn't consider any electrostatic interaction, eventually responsible for the intermolecular interaction and information propagation. To study a more realistic case, we evaluate the molecule charge distribution under the effects of two point charges emulating the presence of a possible driver molecule, see Fig. 8(a). The two driver point charges are fixed to Q_{D1} = 0.8 a.u. and Q_{D2} = 0.2 a.u to emulate the presence of a not fully polarised diallyl butane.

Fig. 8(b) shows the obtained atomic charge in a 500 fs timeframe. It can be seen that point charges induce a net charge separation of the two aggregated charges Q_{DOT1} and Q_{DOT2}, confirming the possible encoding of the binary information. Indeed, the charge configuration is opposite to the one of the driver, correctly propagating the information.

The temperature is firstly considered constant to 5 K. Fig. 8(c) shows the FFT of Q_{DOT1} aggregated charge. Similarly to previous results, the prominence of peaks at near-

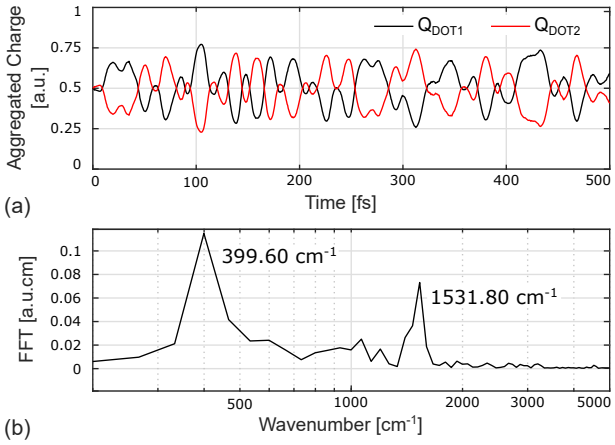

Fig. 6: Dynamics of diallyl butane molecule: (a) DOT1 and DOT2 aggregated charges evaluated with Ab Initio Molecular Dynamics at 350 K. (b) Fast-Fourier Transform (FFT) evaluated for the DOT1 atom charge.

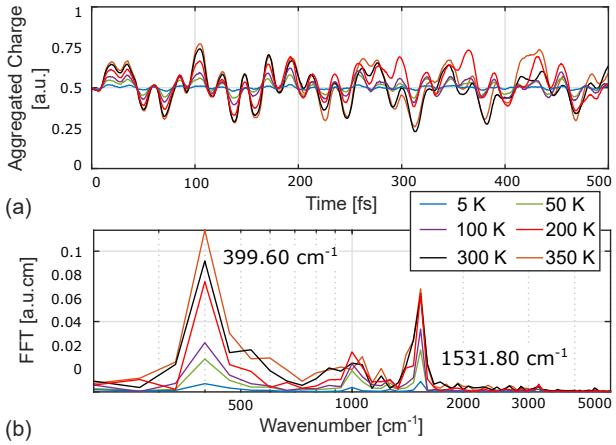

Fig. 7: Diallyl butane molecule: (a) Effect of temperature on the molecule charge distribution. (b) Fast-Fourier Transform (FFT) evaluated for the DOT1 atom charge.

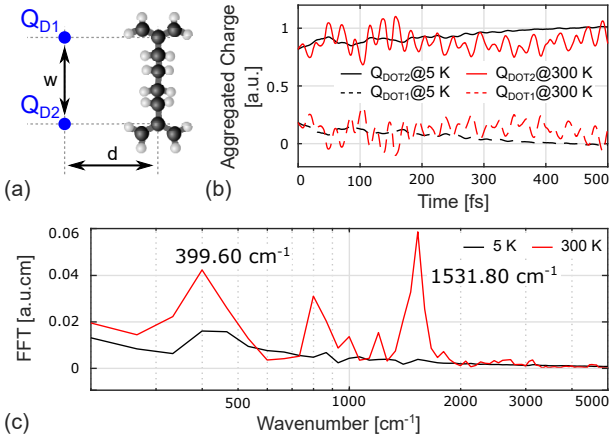

Fig. 8: Effects of electric fields on a diallyl-butane molecule: (a) the point charge system emulates the presence of a driver molecule influencing the charge distribution of the diallyl butane. Charges are positioned at a distance $d = w$ from the molecule under test. (b) Charge distribution of the diallyl butane molecule evaluated under the effect of the driver system with Q_{D1} = 0.2 a.u. and Q_{D2} = 0.8 a.u. at two different temperatures. (c) FFT of the DOT1 charge Q_{DOT1}.

absolute zero temperature is low, and the oscillating components of the charge are suppressed. This demonstrates the robustness of information encoding at a low temperature against molecule vibrations.

When the temperature increases to 300 K, the charge is still well-separated, and the oscillations are limited. It is interesting to see the values of the two-dot charges can become closer, yet they never overlap. Notwithstanding the driver molecule is not fully polarised (the driver molecule is considered fully polarised when Q_{D1} or Q_{D2} is null), the charge of the molecule is well-defined and oscillations do not invert the information. This result represents a step toward the assessment of molecular FCN as a possible candidate for future digital electronics at ambient temperature.

To validate the use of current static transcharacteristics [8], we also analyse the influence of the driver molecule through a single-point calculation with equilibrium geometry, resulting in Q_{DOT1} = 0.1840 a.u. and Q_{DOT2} = 0.8160 a.u.. This result is not far from the average value of aggregated charges obtained in the AIMD calculation, further confirming the validity of static transcharacteristics for the analysis of molecular FCN devices. Notice that the obtained charge separation in the dynamic case is better than the one predicted with the single-point calculation. This implies that a device could encode the information better than predicted with normal static methods. This suggests the transcharacteristics approach naturally underestimates, at least in this particular case, the charge separation of molecules. The robustness of the final molecular design will show results better than expectations and design constraints.

V. Conclusion

Molecular Field-Coupled Nanocomputing (FCN) is one of the most outstanding proposals in the context of Beyond-CMOS technologies. It encodes the information in the charge distribution of molecules and propagates it through electrostatic interaction. The absence of charge transport makes FCN paradigm very promising for very low-power digital electronics. No electric current is present in the propagation of the information, drastically reducing the power dissipation.

Table III. Effect of the electrostatic interaction on diallyl butane.

T [K]	$\bar{Q}_{DOT1}$ [a.u.]	$\bar{Q}_{DOT2}$ [a.u.]	σ_Q [a.u.]
5	0.0610	0.9390	0.0496
300	0.1177	0.8823	0.0806

At the current research state, the modelling and the theoretical analysis of this technology generally rely on the use of geometrical static models which consider the molecule as a set of charges fixed in the space. In a more realistic situation, molecules are affected by molecular vibrations, which make the position of atoms oscillating and moving in the space. This work proposes a methodology, based on Ab Initio Molecular Dynamics, to study the effects of molecular vibrations on the charge distribution of possible FCN molecules. We validate the methodology through the water molecule, then, we study the effects of temperature and electric fields on the 1,4-diallyl butane cation.

Qualitative and quantitative results provide important feedback both from a modelling and a practical perspective. Indeed, the molecular vibrations make the charge of the molecules oscillating about a mean value which is very similar to the static charges obtained by static DFT computation. This results confirm that the use of ab initio evaluated transcharacteristics gives predictions which are robust against molecular vibrations.

The effects of molecular vibrations are studied at several temperatures. The temperature has a direct impact on the amplitude of molecular charge oscillations. The higher is the temperature, the higher is the amplitude of charge oscillations. The diallyl butane has been studied under the influence of a driver molecule to investigate the effects of molecular vibrations in a more realistic situation, thus considering the intermolecular interaction. The results show that the molecule well encodes the binary information. Charge oscillations are present either at near-absolute zero or room temperatures, yet the encoded information never invert. This result makes a step forward in the assessment of molecular FCN technology as a possible candidate for digital electronics working at

ambient temperature.

REFERENCES

[1] C. S. Lent, B. Isaksen, and M. Lieberman, "Molecular quantum-dot cellular automata," *Journal of the American Chemical Society*, vol. 125, no. 4, pp. 1056–1063, 2003, pMID: 12537505. [Online]. Available: https://doi.org/10.1021/ja026856g

[2] Y. Lu and C. S. Lent, "A metric for characterizing the bistability of molecular quantum-dot cellular automata," *Nanotechnology*, vol. 19, no. 15, p. 155703, mar 2008. [Online]. Available: https://doi.org/10.1088%2F0957-4484%2F19%2F15%2F155703

[3] C. S. Lent and P. D. Tougaw, "Lines of interacting quantum-dot cells: A binary wire," *Journal of Applied Physics*, vol. 74, no. 10, pp. 6227–6233, 1993. [Online]. Available: https://doi.org/10.1063/1.355196

[4] K. Walus, T. J. Dysart, G. A. Jullien, and R. A. Budiman, "Qcadesigner: a rapid design and simulation tool for quantum-dot cellular automata," *IEEE Transactions on Nanotechnology*, vol. 3, no. 1, pp. 26–31, March 2004. [Online]. Available: https://doi.org/10.1109/TNANO.2003.820815

[5] S. Srivastava, A. Asthana, S. Bhanja, and S. Sarkar, "Qcapro - an error-power estimation tool for qca circuit design," in *2011 IEEE International Symposium of Circuits and Systems (ISCAS)*, May 2011, pp. 2377–2380. [Online]. Available: https://doi.org/10.1109/ISCAS.2011.5938081

[6] A. Pulimeno, M. Graziano, A. Antidormi, R. Wang, A. Zahir, and G. Piccinini, *Understanding a Bisferrocene Molecular QCA Wire*. Berlin, Heidelberg: Springer Berlin Heidelberg, 2014, pp. 307–338. [Online]. Available: https://doi.org/10.1007/978-3-662-43722-3_13

[7] Y. Ardesi, A. Pulimeno, M. Graziano, F. Riente, and G. Piccinini, "Effectiveness of molecules for quantum cellular automata as computing devices," *Journal of Low Power Electronics and Applications*, vol. 8, no. 3, 2018. [Online]. Available: http://www.mdpi.com/2079-9268/8/3/24

[8] Y. Ardesi, R. Wang, M. Graziano, and G. Piccinini, "Scerpa: a self-consistent algorithm for the evaluation of the information propagation in molecular field-coupled nanocomputing," *IEEE Transactions on Computer-Aided Design of Integrated Circuits and Systems*, vol. 0, p. 0, 2019. [Online]. Available: https://doi.org/10.1109/TCAD.2019.2960360

[9] M. Graziano, R. Wang, M. R. Roch, Y. Ardesi, F. Riente, and G. Piccinini, "Characterisation of a bis-ferrocene molecular qca wire on a non-ideal gold surface," *Micro Nano Letters*, vol. 14, no. 1, pp. 22–27, 2019. [Online]. Available: https://doi.org/10.1049/mnl.2018.5201

[10] Y. Ardesi, L. Gnoli, M. Graziano, and G. Piccinini, "Bistable propagation of monostable molecules in molecular field-coupled nanocomputing," in *2019 15th Conference on Ph.D Research in Microelectronics and Electronics (PRIME)*, July 2019, pp. 225–228. [Online]. Available: https://doi.org/10.1109/PRIME.2019.8787751

[11] F. Riente, G. Ziemys, G. Turvani, D. Schmitt-Landsiedel, S. B. Gamm, and M. Graziano, "Towards logic-in-memory circuits using 3d-integrated nanomagnetic logic," in *2016 IEEE International Conference on Rebooting Computing (ICRC)*, Oct 2016, pp. 1–8. [Online]. Available: https://doi.org/10.1109/ICRC.2016.7738700

[12] U. Garlando, F. Riente, G. Turvani, A. Ferrara, G. Santoro, M. Vacca, and M. Graziano, "Architectural exploration of perpendicular nano magnetic logic based circuits," *Integration*, vol. 63, pp. 275 – 282, 2018. [Online]. Available: http://www.sciencedirect.com/science/article/pii/S0167926017306090

[13] A. Palii, S. Zilberg, A. Rybakov, and B. Tsukerblat, "Double-dimeric versus tetrameric cells for quantum cellular automata: a semiempirical approach to evaluation of cell–cell responses combined with quantum-chemical modeling of molecular structures," *The Journal of Physical Chemistry C*, vol. 123, no. 36, pp. 22 614–22 623, 2019. [Online]. Available: https://doi.org/10.1021/acs.jpcc.9b05942

[14] M. Ottavi, S. Pontarelli, E. P. DeBenedictis, A. Salsano, S. Frost-Murphy, P. M. Kogge, and F. Lombardi, "Partially reversible pipelined qca circuits: Combining low power with high throughput," *IEEE Transactions on Nanotechnology*, vol. 10, no. 6, pp. 1383–1393, Nov 2011. [Online]. Available: http://dx.doi.org/10.1109/TNANO.2011.2147796

[15] M. Awais, M. Vacca, M. Graziano, and G. Masera, "Fft implementation using qca," in *2012 19th IEEE International Conference on Electronics, Circuits, and Systems (ICECS 2012)*, Dec 2012, pp. 741–744. [Online]. Available: http://dx.doi.org/10.1109/ICECS.2012.6463648

[16] P. D. Tougaw and C. S. Lent, "Logical devices implemented using quantum cellular automata," *Journal of Applied Physics*, vol. 75, no. 3, pp. 1818–1825, 1994. [Online]. Available: https://doi.org/10.1063/1.356375

[17] V. Arima, M. Iurlo, L. Zoli, S. Kumar, M. Piacenza, F. Della Sala, F. Matino, G. Maruccio, R. Rinaldi, F. Paolucci, M. Marcaccio, P. G. Cozzi, and A. P. Bramanti, "Toward quantum-dot cellular automata units: thiolated-carbazole linked bisferrocenes," *Nanoscale*, vol. 4, no. 3, pp. 813–823, 2012. [Online]. Available: http://dx.doi.org/10.1039/C1NR10988J

[18] R. Wang, A. Pulimeno, M. Roch, G. Turvani, G. Piccinini, and M. Graziano, "Effect of a clock system on bis-ferrocene molecular qca," *IEEE Transactions on Nanotechnology*, vol. PP, no. 99, pp. 1–1, 2016. [Online]. Available: https://doi.org/10.1109/TNANO.2016.2555931

[19] F. Riente, U. Garlando, G. Turvani, M. Vacca, M. Ruo Roch, and M. Graziano, "Magcad: Tool for the design of 3-d magnetic circuits," *IEEE Journal on Exploratory Solid-State Computational Devices and Circuits*, vol. 3, pp. 65–73, Dec 2017. [Online]. Available: https://doi.org/10.1109/JXCDC.2017.2756981

[20] M. Vacca, S. Frache, M. Graziano, F. Riente, G. Turvani, M. R. Roch, and M. Zamboni, *ToPoliNano: NanoMagnet Logic Circuits Design and Simulation*. Berlin, Heidelberg: Springer Berlin Heidelberg, 2014, pp. 274–306. [Online]. Available: https://doi.org/10.1007/978-3-662-43722-3_12

[21] G. Turvani, A. Tohti, M. Bollo, F. Riente, M. Vacca, M. Graziano, and M. Zamboni, "Physical design and testing of nano magnetic architectures," in *2014 9th IEEE International Conference on Design Technology of Integrated Systems in Nanoscale Era (DTIS)*, May 2014, pp. 1–6. [Online]. Available: http://dx.doi.org/10.1109/DTIS.2014.6850676

[22] A. Pulimeno, M. Graziano, C. Abrardi, D. Demarchi, and G. Piccinini, "Molecular qca: A write-in system based on electric fields," in *The 4th IEEE International NanoElectronics Conference*, June 2011, pp. 1–2. [Online]. Available: https://doi.org/10.1109/INEC.2011.5991702

[23] E. Blair, "Electric-field inputs for molecular quantum-dot cellular automata circuits," *IEEE Transactions on Nanotechnology*, vol. 18, pp. 453–460, 2019. [Online]. Available: https://doi.org/10.1109/TNANO.2019.2910823

[24] F. Neese, "The orca program system," *Wiley Interdisciplinary Reviews: Computational Molecular Science*, vol. 2, no. 1, pp. 73–78, 2012. [Online]. Available: https://onlinelibrary.wiley.com/doi/abs/10.1002/wcms.81

[25] ——, "Software update: the orca program system, version 4.0," *Wiley Interdisciplinary Reviews: Computational Molecular Science*, vol. 8, no. 1, p. e1327, 2018. [Online]. Available: https://onlinelibrary.wiley.com/doi/abs/10.1002/wcms.1327

[26] S. Grimme, J. Antony, S. Ehrlich, and H. Krieg, "A consistent and accurate ab initio parametrization of density functional dispersion correction (dft-d) for the 94 elements h-pu," *The Journal of Chemical Physics*, vol. 132, no. 15, p. 154104, 2010. [Online]. Available: https://doi.org/10.1063/1.3382344

[27] S. Grimme, S. Ehrlich, and L. Goerigk, "Effect of the damping function in dispersion corrected density functional theory," *Journal of Computational Chemistry*, vol. 32, no. 7, pp. 1456–1465, 2011. [Online]. Available: https://onlinelibrary.wiley.com/doi/abs/10.1002/jcc.21759

[28] "Webelements," https://www.webelements.com, accessed: January 2020.

[29] N. F. Zobov, O. L. Polyansky, C. L. Sueur, and J. Tennyson, "Vibration-rotation levels of water beyond the born-oppenheimer approximation," *Chemical Physics Letters*, vol. 260, no. 3, pp. 381 – 387, 1996. [Online]. Available: http://www.sciencedirect.com/science/article/pii/000926149600872X

[30] F. Weigend and R. Ahlrichs, "Balanced basis sets of split valence, triple zeta valence and quadruple zeta valence quality for h to rn: Design and assessment of accuracy," *Physical Chemistry Chemical Physics*, vol. 7, no. 18, p. 3297, 2005. [Online]. Available: https://doi.org/10.1039/b508541a